GFZ
Helmholtz-Zentrum
POTSDAM

Originally published as:

Key Points:
- We found principal changes of the subduction scenarios in different parts of the Arabia-Eurasia collision zone
- In the Western Great Caucasus we propose initiation of subduction polarity reversal
- Counteracting subduction zones are located beneath northwest Zagros in the south and beneath the East Greater Caucasus and Alborz in the north

Supporting Information:
- Supporting Information S1
- Data Set S1

Correspondence to:
M. K. Kaban,
kaban@gfz-potsdam.de

Diverse Continental Subduction Scenarios Along the Arabia-Eurasia Collision Zone

Mikhail K. Kaban[1,2] (iD), **Alexey G. Petrunin**[1,2] (iD), **Sami El Khrepy**[3,4], and **Nassir Al-Arifi**[3]

[1]German Research Centre for Geosciences (GFZ), Potsdam, Germany, [2]Institute of Physics of the Earth, Russian Academy of Sciences, Moscow, Russia, [3]Geology and Geophysics Department, King Saud University, Riyadh, Saudi Arabia, [4]National Research Institute of Astronomy and Geophysics, NRIAG, Helwan, Egypt

Abstract It is generally accepted that convergence of the Arabian and African plates is a subduction-dominated process. However, the subduction scenarios are still debatable. Here we present a 3-D model of the mantle to a depth of 700 km, based on a joint interpretation of the seismic tomography, residual topography, residual mantle gravity field, and seismicity. At the northwestern edge of the collision zone, we only observe partial underthrust of the Eurasian plate under the West Greater Caucasus. We suggest that this is the initial stage of subduction polarity reversal after the break off of the plate formerly subducted northward. To the southeast, counteracting subduction zones are found beneath northwest Zagros in the south and beneath the East Greater Caucasus and Alborz in the north. This scenario is likely the result of highly buoyant and weak blocks of the Lesser Caucasus, Alborz, and northwest Zagros, which are underlain in the south by the Arabian plate and the Scythian plate and South Caspian from the opposite side. Further to the southeast, a delaminated lithospheric slab is observed under southeast Zagros, while the Arabian and Eurasian plates only partially underthrust East Zagros and Kopet Dagh, respectively. In the southern part of the collision zone under Makran, only remnants of the formerly subducted slabs are found below 200 km.

Plain Language Summary Continental collision zones are a result of plate tectonics on the planet Earth, when moving lithospheric plates collide at convergent boundaries. This process causes enormous concentration of deformations and stresses leading to increased seismic activity and large earthquakes, which can destroy entire cities. On the other hand, the collision process may also lead to formation of large sedimentary basins bearing ore and hydrocarbon deposits. Therefore, understanding of the mechanisms governing this process is crucial for human habitat. It is generally accepted that convergence of the Arabian and Eurasian plates is a subduction-dominated process, when one plate penetrates under another along an inclined subduction zone. However, the subduction scenarios are still debatable. Here, we present a 3-D model of the mantle to a depth of 700 km, based on a joint interpretation of various geophysical data. For the first time, we demonstrate an image of the counter-acting subduction zones beneath Zagros in the South and beneath the East Greater Caucasus and Alborz in the North. This observation contradicts the conventional view of the northward subduction at the northern flank of the Arabia-Eurasia plate boundary. These results have important implications for the debates concerning evolution and dynamics of continental collision zones.

1. Introduction

The Arabia-Eurasia continental collision zone is one of the largest and most active, both seismically and tectonically, on Earth. The Greater and Lesser Caucasus form the northwestern rim of the collision zone (Ruban et al., 2007; Figure 1a). The northeastern border is delineated by the Kopet Dagh and Afghan terranes, which are separated from the Caucasus by the strong South Caspian block (Allen et al., 2002). The latter is bounded by the Alborz terrain in the south. The southwestern boundary of the collision zone is presented by the East Anatolian block and Bitlis Suture Zone, which continue into the Zagros folded belt and to Makran at the southeastern rim. The Iranian plateau and the Lut block are in the central part of the collision zone. Subduction has long been considered a dominant process, which accommodates convergence of the plates. However, scenarios of this process at different points on the convergent boundaries are highly debated. Up to now, most of the models are based on the upper crust/surface geological observations (e.g., structural and stratigraphic history of the range; e.g., Forte et al., 2014; Saintot et al., 2006), which provide an indirect evidence for the deep tectonic structure of the region and might relate to past tectonic history but not to the
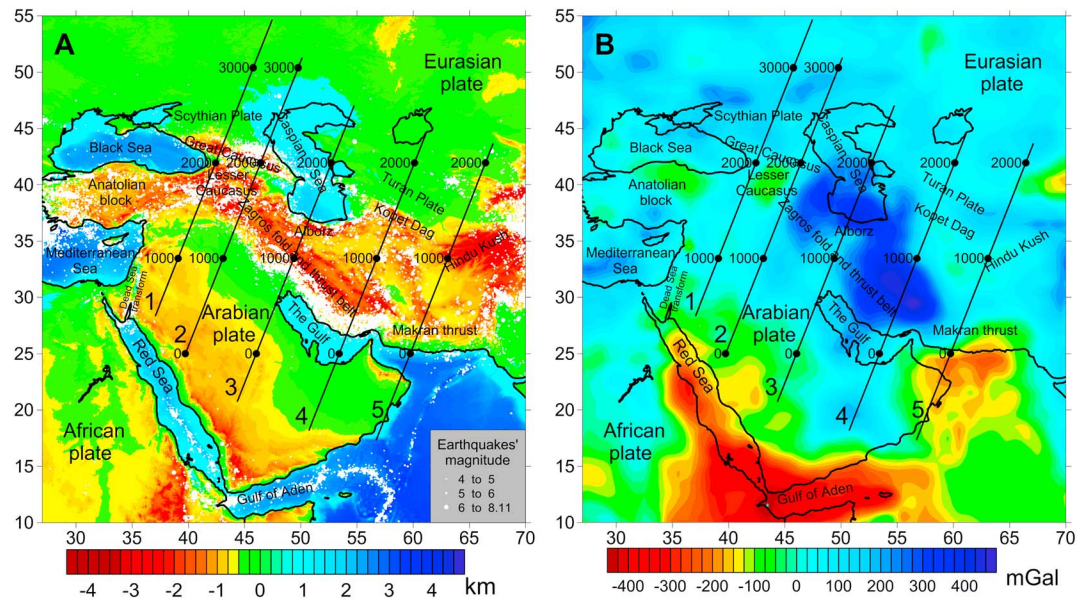
Figure 1. Study area. (a) Topography/bathymetry. White dots show epicenters of earthquakes (earthquake catalogue 1900–2009; Storchak et al., 2013). (b) Residual mantle gravity anomalies showing gravity field of the upper mantle density variations (Kaban, El Khrepy, et al., 2016). Black lines correspond to cross sections discussed in text.

current stage. Meanwhile, it has been demonstrated in modeling studies (both numerical and analogue; e.g., Beaumont & Quinlan, 1994; Butler et al., 2013; Ellis & Beaumont, 2000; Pysklywec, 2001; Willingshofer et al., 2013) that continental subduction leads to formation of a somewhat symmetrical fault system, which includes both prowedge and retrowedge in the crust on the opposite sides of the orogenic belt. This system also includes proforeland and retroforeland basins (e.g., Hoth et al., 2008). However, most of these models are 2-D, while in 3-D case the internal tectonic structure might be even much more complex. Therefore, it is difficult to construct a comprehensive model of the orogenic belt solely based on the surface geology results.

In most studies, the northward subduction of different styles is considered the prevalent process, a result of the long history of convergence and northward subduction of the Neo-Tethys Ocean from at least 150 Ma (e.g., Agard et al., 2011). It is often discussed that the Arabia-Eurasia collision is associated with two subduction zones. In the south, the Arabian lithosphere is subducting under the Zagros fold belt (e.g., Mouthereau et al., 2012). In the north, a potential subduction zone is associated with the Greater Caucasus, South Caspian, and Kopet Dagh (e.g., Mumladze et al., 2015; Vernant et al., 2004). The Arabian-Eurasian collision zone is characterized by a high level of continuing seismic activity, which has been documented historically and instrumentally according to earthquake catalogs (1900–2009; e.g., Storchak et al., 2013), especially associated with plate boundaries (Figure 1). The concentrated NW-SE and NE-SW seismic trends indicate highly deformed well-developed faults associated with different levels and magnitudes of seismicity. It is also worth mentioning that the depth of the earthquake hypocenters varies from the upper crust to much deeper. Most of the hypocenters are located within the crust; however, deep earthquakes with focal depths up to 200 km are also observed in several clusters (Figure 2, section 4). The wide range of these earthquakes' depths reflects strong heterogeneity in the Earth's interior, in particular related to active subduction. Strike-slip and especially thrust faulting has been documented by different styles of focal mechanism solutions at a wide range of hypocenter depths. The absence of seismic activity deeper than 200 km could be due to the slow rate of subduction and aseismic creep-type deformation.

Previously, principal conclusions about the structure of the upper mantle in this region were chiefly based on seismic tomography results. However, seismic velocities do not always provide a complete image of the deep interior as they are mainly affected by temperature variations and less so by composition (e.g., Stixrude & Lithgow-Bertelloni, 2005). Density variations are highly sensitive to both temperature and composition; however, interpretation of the gravity field only is essentially an ill-posed problem. Therefore, usually one or two
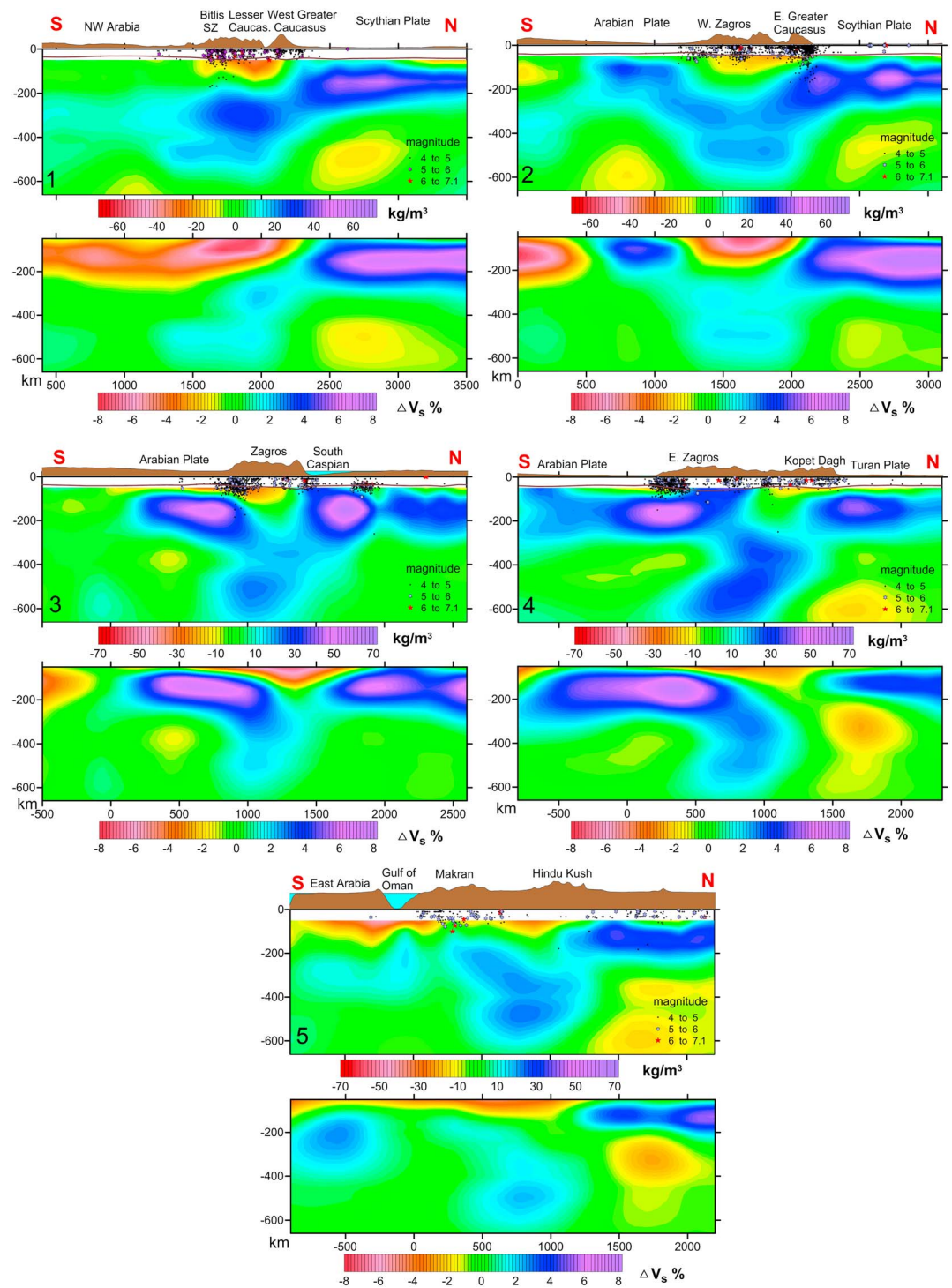
Figure 2. Density and seismic velocity (V_s) variations for five profiles crossing the northwestern part of the Arabia-Eurasia collision zone (Figure 1). The density variations (upper section) are the result of a joint inversion of the seismic tomography model, residual topography, and residual mantle gravity field. The earthquakes are collected from Storchak et al. (2013). The S wave velocity variations of Schaeffer and Lebedev (2013) are shown in the bottom.

parameters only are determined in such kind of studies. For example, Motavalli-Anbaran et al. (2016), studying a part of the Arabia-Eurasia collision zone with limited constraints on the crustal structure determination, restricted their gravity inversion to the Moho and LAB depth determinations. In the present

study, we use a joint inversion of seismic tomography, residual (crust-free) gravity anomalies (Figure 1b), and residual topography to produce a 3-D density model of the mantle to a depth of 700 km (Kaban, El Khrepy, et al., 2016). Using different geophysical fields provides a possibility of revealing the structure of the upper mantle much more comprehensively than ever before. Based on this model, we analyze the results for several profiles across the collision zone, which demonstrate the principal variations of the continental subduction scenarios from the northwestern flank of the collision zone to the southeastern flank.

2. Method and Data

To determine density variations in the upper mantle, we used three principal data sets: (i) *S* wave variations from the tomography model of Schaeffer and Lebedev (2013), (ii) residual topography, and (iii) mantle gravity anomalies (Kaban, El Khrepy, et al., 2016). The residual topography and residual gravity anomalies are resulting from extraction of the crustal influence both from the observed gravity field and from the surface topography/bathymetry. Additionally, we have also removed the effect of the lower mantle based on global dynamics models (see Kaban, El Khrepy, et al., 2016; Kaban et al., 2015, for more details). Thus, the resulting fields represent a segregated effect of the density heterogeneities in the upper mantle. The *S* wave variations were converted to density variations, which we employed as the initial approximation. Above 300 km, we used the initial density model of Kaban et al. (2016), which is based on the mineral physics approach (Tesauro et al., 2014). For the depth interval of 300–700 km, a constant scaling factor d (ln$\Delta\rho$)/d (lnΔVs) = 0.28 was applied to convert velocity variations into density variations (Kaban et al., 2015).

The residual gravity and topography were inverted together with the initial density model to obtain the final density variations in the upper mantle using the method firstly developed for studying North America (Kaban et al., 2015). The objective function aims to minimize, in terms of the least squares, both parameters (the residual topography and gravity variations). Since the residual topography and gravity depend differently on the size, amplitude, and depth of the primary density anomaly, the calculated 3-D density structure employing both these parameters provides much better resolution, especially with depth, compared to the models based on the gravity field inversion only (Kaban et al., 2015). To stabilize the inversion, we used the Occam's principle; namely, we looked for a solution with minimal deviations from the initial model. The maximal horizontal resolution of the final model is about 150 km and vertical −50 km.

This technique was tested extensively on synthetic models (Kaban et al., 2015). It has been demonstrated that with the joint inversion of the residual gravity and topography, it is possible to locate various kinds of anomalous structures, in particular—inclined high-density slabs even without considering additional information provided by seismic tomography. Although the amplitude of the reconstructed density anomalies might be reduced by damping, their shape and location are restored correctly. This has been proven by previous results obtained for western Pacific. The subduction zone in the Ryukyu and Marianna arcs was indistinguishable in the initial seismic tomography model but became visible after the joint inversion with the residual mantle gravity and topography (Kaban, Stolk, et al., 2016).

Although this technique was employed earlier for different regions (e.g., Kaban, El Khrepy, et al., 2016), in this study we have expanded the model to a depth of 700 km in contrast to 300 km, which was the depth limit in the aforementioned paper. This gives a view on configuration of the subducting slabs down to the bottom of the transition zone. The more detailed descriptions of the method including the model setup, main procedure, description of parameters, and stability tests are provided in Kaban et al. (2016).

3. Results

Here we show the results for the five profiles, which demonstrate the transformation of the upper mantle structure across the Arabia-Eurasia collision zone from the northwest to southeast (Figure 1). The calculated density variations to a depth of 660 km are shown in Figure 2. The variations of *S* wave velocities according to the model of Schaeffer and Lebedev (2013) are shown in the final density cross sections (Figure 2). Three principal factors responsible for the modification of the initial tomography-based model should be emphasized. First, the resolution of the initial model has been improved in the inversion. Second, the joint inversion reveals density heterogeneity, which is not clearly reflected by seismic tomography. Primarily, these are composition variations, which strongly affect density but not seismic velocities. With respect to the subduction process, this might be a result of a large volume of eclogite in the subducting plate, which is characterized
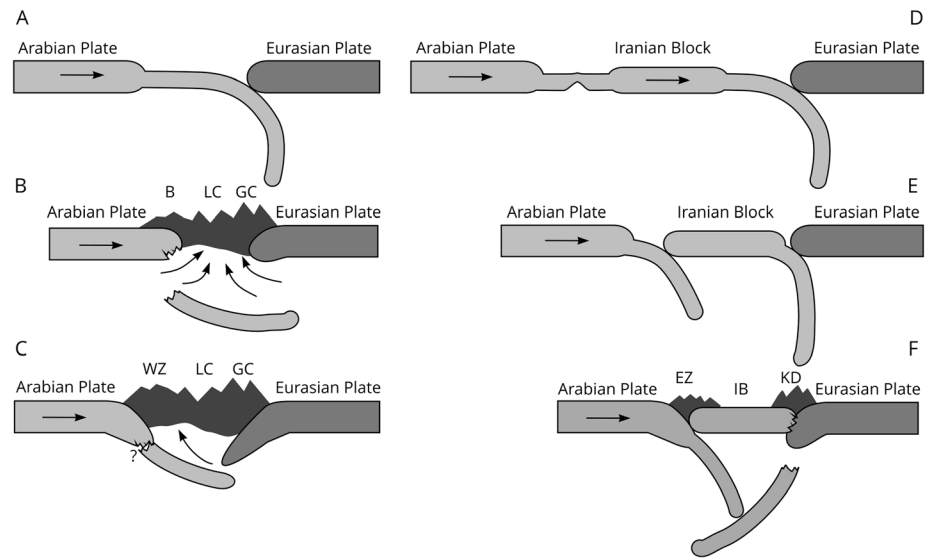
Figure 3. Cartoons illustrating geodynamic models for the western (a–c) and eastern (d–f) parts of the Arabia-Eurasia collision zone. (a) and (d) correspond to a precollisions stage of the closing of Neo-Tethys. (b) West Great Caucasus (GC, profile 1, Figure 2): Delamination of the formerly subducted slab is followed by uprising of the hot asthenospheric material under the Lesser Caucasus (LC) and initiation of underthrusting of the Eurasian plate under the West GC. (c) East Great Caucasus (profile 2, Figure 2): underthrusting of the Arabian plate under West Zagros (WZ), partial delamination of the Neo-Thetis plate, well-developed underthrust of the Eurasian plate under the East GC. (e) Convergence of the Iranian block (IB) with Eurasia, development of the subduction zone at the southern flank of the IB, bending of the northern subducting plate (e.g., Ribe, 2010). (f) corresponds to profile 4, Figure 2: underthrust of the Arabian plate under East Zagros (EZ) and IB in conjunction with the detached plate, partial underthrust of the Eurasian plate under Kopet Dagh.

by a very high density, which exceeds by up to 60 kg/m^3 the reference density at the same depth. Third, the corrected density variations account for the factors not considered in the initial velocity-to-density conversion, such as the presence of volatiles, which strongly affect seismic velocities (e.g., Cammarano et al., 2003).

3.1. Northwestern Part of the Arabia-Eurasia Collision Zone

The northwestern part of the collision zone is represented by the Great Caucasus in the North and the Bitlis Suture Zone with Western Zagros in the south (Figure 1). Section 1 (Figure 2) crosses the westernmost part of the collision zone: from the northwestern Arabian plate to the Scythian plate through the Bitlis Suture Zone, Lesser Caucasus, and the West Greater Caucasus (Figure 2, section 1). In the southern edge, we do not see any evidence for ongoing subduction of the Arabian plate under the Bitlis Suture Zone. A high-density body is observed below 200 km, which partially penetrates the transition zone. We interpret this body as a remnant of the formerly subducted slab. The material of this dense lithosphere block might be eclogitized because it is not well expressed in the initial tomography model. However, this might be also due to insufficient resolution of the last one. This finding is in agreement with previous seismic studies and geodynamic modeling (e.g., Faccenna et al., 2006; Lei & Zhao, 2007). The uppermost mantle is characterized by very low densities, which is likely a result of penetration of the hot asthenospheric material in the slabless window after the delamination of the formerly subducted slab (Figure 3b) in agreement with previous results of Göğüş and Pysklywec (2008a, 2008b).

For the northern edge, most of the authors argue for a northward dipping slab under Western Great Caucasus, which originates from the closure of the former back-arc basin (e.g., Vernant et al., 2004) or the absence of present-day subduction after delamination of the formerly subducted slab (e.g., Forte et al., 2014; Mumladze et al., 2015). The last conclusion is also supported by local tomography studies (Koulakov et al., 2012) and rheological models indicating very low effective elastic thickness of the lithosphere in the Western Great Caucasus (Chen et al., 2015; Ruppel & McNutt, 1990). Therefore, it is unlikely that this weak and highly buoyant lithosphere can dip under the strong, thick, and dense lithosphere in the north. In

contrast, the obtained density model along the first profile clearly shows at least partial underthrust of the Scythian plate under the Western Greater Caucasus (Figure 2, section 1). This underthrust is already visible in the initial tomography model, but the amplitude of the adjusted density variations is much prominent. However, we do not observe deep seismicity under the Western Great Caucasus, which should accompany possible southward subduction, only diffused crustal seismicity is presented in this structure (Figure 2, section 1). It is also important that geological studies do not find any structures in the northern half of the Western Greater Caucasus, which correspond to a north dipping limb of a crustal scale anticline (e.g., Forte et al., 2014; Saintot et al., 2006). On the other hand, geochemical and isotope analysis at the Elbrus (northern flank of the West Great Caucasus) and Kazbek (Central Great Caucasus) volcanoes showed low He isotope ratios and Sr-Nd-Pb signatures, which evidence for magma sources from mixture of the parental mantle and continental crust (Lebedev et al., 2010). This might be an argument for the ongoing underthrusting of the Scythian plate below the Great Caucasus. To explain these controversial results, we hypothesize that presently, we observe an initial stage of flipping the subduction polarity, which may follow the plate break off (e.g., Teng et al., 2000). The slabless window under the Western Great Caucasus provides conditions for overthrusting the thick and dense Scythian plate by this structure; however, this process has just been initiated due to a very low plate convergence rate (e.g., Forte et al., 2014).

As it was proposed earlier, the subduction polarity reversal might be explained by the ablation of the formerly subducted slabs with continuous convergence of the continental lithosphere (e.g., Tao & O'connell, 1992). Although this study relates to younger oceanic plates, it was revealed that a flip of the subduction polarity can be also the case for continental collision zones (e.g., Pysklywec, 2001) as in the continental plate convergence across South Island, New Zealand (Pysklywec et al., 2010). Another example is the subduction polarity reversal between the Western Alps and the Northern Apennines (Handy et al., 2015; Vignaroli et al., 2008). Several historical examples have been proposed as the Neoarchean subduction polarity reversal in the North China Craton (Wang et al., 2015) or the Grampian event in Scotland when the southeastward subduction of the oceanic plate was followed by the northwestward subduction of the Caledonian orogeny (Mitchell, 1978).

When moving to the east, the upper mantle structure drastically changes; we observe a v-shaped density anomaly that might be interpreted as two oppositely directed subducted slabs, dipping to the north under the Zagros fold belt and to the south—under the East Greater Caucasus (Figure 2, section 2). The northward dipping subduction of the Arabian plate under Zagros is well documented by various studies (e.g., Agard et al., 2011); however, for the East Greater Caucasus most of the authors also show a preference of a northward subduction, which has been inherited from the Neo-Tethys (e.g., Mumladze et al., 2015). Principal differences between the Western and Eastern Great Caucasus have been widely discussed in previous studies. Contrary to the Western Great Caucasus, the Eastern is characterized by the strong lithosphere with high effective elastic thickness (Chen et al., 2015; Ruppel & McNutt, 1990). The central (most elevated) part of the East Great Caucasus is a doubly vergent wedge with similar convergence rates on both flanks (e.g., Forte et al., 2014). Therefore, it represents a classical example of the Prowedge-Uplifted Plug-Retrowedge-Conduit model of the continental subduction (e.g., Butler et al., 2013). Our results show that the Eurasian plate (conduit) is dipping southward under the East Great Caucasus (Figure 3c). The deep penetration of the strong Eurasian plate in the upper mantle can be compared with subduction of the old Australian lithosphere (including part of the crust) under the Banda arc to the depth more than 100 km (Fichtner et al., 2010). The deep earthquakes (up to a depth of 200 km) under the northern flank of the East Great Caucasus are clearly related to the upper part of the southward-subducting plate (Figure 2, section 2). This plate, which is characterized by high effective elastic thickness, elastically supports the ridge. Therefore, following Forte et al. (2014), we suggest that the Eastern Great Caucasus corresponds to the next stage of development compared to the Western one, however with the subduction polarity reversal.

3.2. Central Part of the Collision Zone

Further to the southeast, the lithosphere structure is similar to the second profile, although the amplitude of the density anomaly under Zagros and the South Caspian is significantly increased. We observe a counteracting subduction plates at the northern and southern boundaries of the collision zone (Figure 2, section 3). As noted in previous papers, the positive anomaly under the South Caspian may be explained by a

significant volume of eclogites (e.g., Kaban, El Khrepy, et al., 2016). Up to now, different subduction scenarios have been discussed for this structure. Mouthereau et al. (2012) argued for the subduction of the South Caspian block to the north under the Apsheron Sill. In contrast, Axen et al. (2001) noted that a strong uplift of Alborz (~10 km) is synchronous with a quick subsidence of the South Caspian block, which is evidence of subduction of the latter under the buoyant Alborz lithosphere. Our results show that both scenarios might take place, which is in agreement with the seismicity distribution (Figure 2, section 3). In the North, we also see some underthrust of the South Caspian block; however, it is not so significant as in the south. We likely observe initiation of detachment of the lithospheric slab under Zagros; however, this process is far from being completed in this area as hypothesized by Mouthereau et al. (2012). The seismicity pattern (Figure 2, section 3) clearly shows three distinct clusters of deformation. Southern cluster is located beneath Zagros folding zone and characterized by deep (up to 200 km) seismicity that might be an evidence for the subduction-related tectonics. In contrast, two other clusters bounding the South Caspian block are more shallow indicating zones of high strain rates due to strain localization under compressional environment.

3.3. Southeastern Part of the Arabia-Eurasia Collision Zone

In the southeastern part of the collisions zone (Figure 1a, sections 4 and 5), the lithospheric structure changes again. We observe a partially detached high-density block in the transition zone under Zagros likely representing a part of the formerly subducted ocean lithosphere apparently attached to the Arabian plate (Figure 2, section 4). This profile manifests further changes in the present-day collision mechanism (which already might be visible at Figure 2, section 3) with cessation of the active subduction and delamination of the formerly subducted slab (Figure 2, sections 4 and 5, and 3f) that is also supported by the absence of deep earthquakes at these cross sections. This finding is in agreement with the criteria of Göğüş and Pysklywec (2008a, 2008b), such as the low densities in the uppermost mantle and asymmetrical density structure (Figure 2, section 4), which evidence rather for delamination than for dripping of the mantle lithosphere (Figure 3f).

The continuous lithospheric plate is subducting under Zagros to the bottom of the transition zone in conjunction with the detached plate (Figure 2, sections 3 and 5, and 3f). In the southeastern part under Makran, the subducted slab is fully detached from the Arabian plate and we observe only a remnant of the lithospheric plate at depths below 150 km (Figure 2, sections 4 and 5). To the northeast, under the Kopet Dagh and further to the east, only partial underthrust of the Eurasian plate is found (Figure 2, sections 4 and 5). This finding agrees with the flexural model of the Turan Plate being deformed under the loading of the Kopet Dagh (Artemjev & Kaban, 1994).

4. Conclusions

1. We present a 3-D density model of the mantle to a depth of 700 km for the Arabia-Eurasian collision zone and its surroundings. The model is constrained by the seismic tomography, residual topography, residual mantle gravity field, and seismicity. Taking into account different geophysical fields, this model better conveys the upper mantle structure compared to previous studies based on a single method.
2. The results demonstrate principal variations in the continental subduction scenarios from northwest to southeast along the Arabia-Eurasia collision zone.
3. At the northwestern edge of the collision zone, the Scythian plate partially underthrusts the West Greater Caucasus. Taking into account the lack of surface geology evidence of this process, we hypothesize that this is the initial stage of the subduction polarity reversal after the break off of the plate formerly subducted northward. The ablation of the formerly subducted slabs can stimulate the subduction polarity reversal. In the southern edge of this part of the collision zone, a remnant of the delaminated slab is located at a depth below 200 km.
4. Double-sided counteracting subduction is observed in the central part of the collision zone, which is bounded by northwest Zagros in the south and by the East Greater Caucasus and South Caspian in the north. It can be suggested that the East Great Caucasus represents the next stage following the subduction polarity reversal compared to the West Great Caucasus. The buoyant and weak blocks of the Lesser Caucasus, Alborz, and northwest Zagros, forming an orogenic wedge, are underlain by dipping lithospheric plates from both sides.

5. Further to the southeast, the subduction ceased and a detached plate is observed under the southeast rim of Zagros. The Arabian and Eurasian plates only partially underthrust East Zagros from the south and the Kopet Dagh from the north.

References

Agard, P., Omrani, J., Jolivet, L., Whitechurch, H., Vrielynck, B., Spakman, W., et al. (2011). Zagros orogeny: A subduction-dominated process. *Geological Magazine*, *148*(5–6), 692–725. https://doi.org/10.1017/S001675681100046X

Allen, M. B., Jones, S., Ismail-Zadeh, A., Simmons, M., & Anderson, L. (2002). Onset of subduction as the cause of rapid Pliocene-Quaternary subsidence in the South Caspian basin. *Geology*, *30*(9), 775–778. https://doi.org/10.1130/0091-7613(2002)030<0775:OOSATC>2.0.CO;2

Artemjev, M. E., & Kaban, M. K. (1994). Density inhomogeneities, isostasy and flexural rigidity of the lithosphere in the Transcaspian region. *Tectonophysics*, *240*(1–4), 281–297. https://doi.org/10.1016/0040-1951(94)90276-3

Axen, G. J., Lam, P. S., Grove, M., Stockli, D. F., & Hassanzadeh, J. (2001). Exhumation of the west-central Alborz Mountains, Iran, Caspian subsidence, and collision-related tectonics. *Geology*, *29*(6), 559–562. https://doi.org/10.1130/0091-7613(2001)029<0559:EOTWCA>2.0.CO;2

Beaumont, C., & Quinlan, G. (1994). A geodynamic framework for interpreting crustal scale seismic reflectivity patterns in compressional orogens. *Geophysical Journal International*, *116*(3), 754–783. https://doi.org/10.1111/j.1365-246X.1994.tb03295.x

Butler, J. P., Beaumont, C., & Jamieson, R. A. (2013). The Alps 1: A working geodynamic model for burial and exhumation of (ultra) high-pressure rocks in Alpine-type orogens. *Earth and Planetary Science Letters*, *377*, 114–131.

Cammarano, F., Goes, S., Vacher, P., & Giardini, D. (2003). Inferring upper-mantle temperatures from seismic velocities. *Physics of the Earth and Planetary Interiors*, *138*, 197–222. https://doi.org/10.1016/S0031-9201(03)00156-0

Chen, B., Kaban, M. K., El Khrepy, S., & Al-Arifi, N. (2015). Effective elastic thickness of the Arabian plate: Weak shield versus strong platform. *Geophysical Research Letters*, *42*, 3298–3304. https://doi.org/10.1002/2015GL063725

Ellis, S., & Beaumont, C. (2000). Models of convergent boundary tectonics: Implications for the interpretation of Lithoprobe data. *Canadian Journal of Earth Sciences*, *36*(10), 1711–1741.

Faccenna, C., Bellier, O., Martinod, J., Piromallo, C., & Regard, V. (2006). Slab detachment beneath eastern Anatolia: A possible cause for the formation of the North Anatolian fault. *Earth and Planetary Science Letters*, *242*(1–2), 85–97. https://doi.org/10.1016/j.epsl.2005.11.046

Fichtner, A., De Wit, M., & van Bergen, M. (2010). Subduction of continental lithosphere in the Banda Sea region: Combining evidence from full waveform tomography and isotope ratios. *Earth and Planetary Science Letters*, *297*(3–4), 405–412. https://doi.org/10.1016/j.epsl.2010.06.042

Forte, A. M., Cowgill, E., & Whipple, K. X. (2014). Transition from a singly vergent to doubly vergent wedge in a young orogen: The Greater Caucasus. *Tectonics*, *33*, 2077–2101. https://doi.org/10.1002/2014TC003651

Göğüş, O. H., & Pysklywec, R. N. (2008a). Mantle lithosphere delamination driving plateau uplift and synconvergent extension in eastern Anatolia. *Geology*, *36*(9), 723–726. https://doi.org/10.1130/G24982A.1

Göğüş, O. H., & Pysklywec, R. N. (2008b). Near-surface diagnostics of dripping or delaminating lithosphere. *Journal of Geophysical Research*, *113*, B11404. https://doi.org/10.1029/2007JB005123

Handy, M. R., Ustaszewski, K., & Kissling, E. (2015). Reconstructing the Alps–Carpathians–Dinarides as a key to understanding switches in subduction polarity, slab gaps and surface motion. *International Journal of Earth Sciences*, *104*(1), 1–26. https://doi.org/10.1007/s00531-014-1060-3

Hoth, S., Kukowski, N., & Oncken, O. (2008). Distant effects in bivergent orogenic belts—How retro-wedge erosion triggers resource formation in pro-foreland basins. *Earth and Planetary Science Letters*, *273*(1–2), 28–37. https://doi.org/10.1016/j.epsl.2008.05.033

Kaban, M. K., El Khrepy, S., Al-Arifi, N., Tesauro, M., & Stolk, W. (2016). Three-dimensional density model of the upper mantle in the Middle East: Interaction of diverse tectonic processes. *Journal of Geophysical Research: Solid Earth*, *121*, 5349–5364. https://doi.org/10.1002/2015JB012755

Kaban, M. K., Mooney, W. D., & Petrunin, A. G. (2015). Cratonic root beneath North America shifted by basal drag from the convecting mantle. *Nature Geoscience*, *8*(10), 797–800. https://doi.org/10.1038/ngeo2525

Kaban, M. K., Stolk, W., Tesauro, M., El Khrepy, S., Al-Arifi, N., Beekman, F., & Cloetingh, S. A. P. L. (2016). 3D density model of the upper mantle of Asia based on inversion of gravity and seismic tomography data. *Geochemistry, Geophysics, Geosystems*, *17*, 4457–4477. https://doi.org/10.1002/2016GC006458

Koulakov, I., Zabelina, I., Amanatashvili, I., & Meskhia, V. (2012). Nature of orogenesis and volcanism in the Caucasus region based on results of regional tomography. *Solid Earth*, *3*(2), 327–337. https://doi.org/10.5194/se-3-327-2012

Lebedev, V. A., Chernyshev, I. V., Chugaev, A. V., Gol'tsman, Y. V., & Bairova, E. D. (2010). Geochronology of eruptions and parental magma sources of Elbrus volcano, the Greater Caucasus: K-Ar and Sr-Nd-Pb isotope data. *Geochemistry International*, *48*(1), 41–67. https://doi.org/10.1134/S0016702910010039

Lei, J., & Zhao, D. (2007). Teleseismic evidence for a break-off subducting slab under Eastern Turkey. *Earth and Planetary Science Letters*, *257*(1–2), 14–28. https://doi.org/10.1016/j.epsl.2007.02.011

Mitchell, A. H. G. (1978). The Grampian orogeny in Scotland: Arc-continent collision and polarity reversal. *The Journal of Geology*, *86*(5), 643–646. https://doi.org/10.1086/649729

Motavalli-Anbaran, S. H., Zeyen, H., & Jamasb, A. (2016). 3D crustal and lithospheric model of the Arabia–Eurasia collision zone. *Journal of Asian Earth Sciences*, *122*, 158–167. https://doi.org/10.1016/j.jseaes.2016.03.012

Mouthereau, F., Lacombe, O., & Vergés, J. (2012). Building the Zagros collisional orogen: Timing, strain distribution and the dynamics of Arabia/Eurasia plate convergence. *Tectonophysics*, *532*, 27–60.

Mumladze, T., Forte, A. M., Cowgill, E. S., Trexler, C. C., Niemi, N. A., Yıkılmaz, M. B., & Kellogg, L. H. (2015). Subducted, detached, and torn slabs beneath the Greater Caucasus. *GeoResJ*, *5*, 36–46. https://doi.org/10.1016/j.grj.2014.09.004

Pysklywec, R. N. (2001). Evolution of subducting mantle lithosphere at a continental plate boundary. *Geophysical Research Letters*, *28*(23), 4399–4402. https://doi.org/10.1029/2001GL013567

Pysklywec, R. N., Gogus, O., Percival, J., Cruden, A. R., & Beaumont, C. (2010). Insights from geodynamical modeling on possible fates of continental mantle lithosphere: Collision, removal, and overturn. *Canadian Journal of Earth Sciences*, *47*(4), 541–563. https://doi.org/10.1139/E09-043

Ribe, N. M. (2010). Bending mechanics and mode selection in free subduction: A thin-sheet analysis. *Geophysical Journal International*, *180*(2), 559–576. https://doi.org/10.1111/j.1365-246X.2009.04460.x

Ruban, D. A., Al-Husseini, M. I., & Iwasaki, Y. (2007). Review of Middle East Paleozoic plate tectonics. *GeoArabia-MANAMA*, *12*(3), 35.

Ruppel, C., & McNutt, M. (1990). Regional compensation of the Greater Caucasus mountains based on an analysis of Bouguer gravity data. *Earth and Planetary Science Letters*, *98*(3–4), 360–379. https://doi.org/10.1016/0012-821X(90)90037-X

Saintot, A., Brunet, M. F., Yakovlev, F., Sébrier, M., Stephenson, R., Ershov, A., et al. (2006). The Mesozoic-Cenozoic tectonic evolution of the Greater Caucasus. *Geological Society, London, Memoirs*, *32*(1), 277–289. https://doi.org/10.1144/GSL.MEM.2006.032.01.16

Schaeffer, A. J., & Lebedev, S. (2013). Global shear-speed structure of the upper mantle and transition zone. *Geophysical Journal International*, *194*(1), 417–449. https://doi.org/10.1093/gji/ggt095

Stixrude, L., & Lithgow-Bertelloni, C. (2005). Thermodynamics of mantle minerals—I. Physical properties. *Geophysical Journal International*, *162*, 610–632.

Storchak, D. A., Di Giacomo, D., Bondár, I., Engdahl, E. R., Harris, J., Lee, W. H. K., et al. (2013). Public release of the ISC-GEM global instrumental earthquake catalogue (1900–2009). *Seismic Research Letters*, *84*(5), 810–815. https://doi.org/10.1785/0220130034

Tao, W. C., & O'connell, R. J. (1992). Ablative subduction: A two-sided alternative to the conventional subduction model. *Journal of Geophysical Research*, *97*(B6), 8877–8904. https://doi.org/10.1029/91JB02422

Teng, L. S., Lee, C. T., Tsai, Y. B., & Hsiao, L. Y. (2000). Slab breakoff as a mechanism for flipping of subduction polarity in Taiwan. *Geology*, *28*(2), 155–158. https://doi.org/10.1130/0091-7613(2000)28<155:SBAAMF>2.0.CO;2

Tesauro, M., Kaban, M. K., Mooney, W. D., & Cloetingh, S. A. P. L. (2014). Density, temperature, and composition of the North American lithosphere—New insights from a joint analysis of seismic, gravity, and mineral physics data: 2. Thermal and compositional model of the upper mantle. *Geochemistry, Geophysics, Geosystems*, *15*(12), 4808–4830. https://doi.org/10.1002/2014GC005484

Vernant, P., Nilforoushan, F., Hatzfeld, D., Abbassi, M. R., Vigny, C., Masson, F., et al. (2004). Present-day crustal deformation and plate kinematics in the Middle East constrained by GPS measurements in Iran and northern Oman. *Geophysical Journal International*, *157*(1), 381–398. https://doi.org/10.1111/j.1365-246X.2004.02222.x

Vignaroli, G., Faccenna, C., Jolivet, L., Piromallo, C., & Rossetti, F. (2008). Subduction polarity reversal at the junction between the Western Alps and the Northern Apennines, Italy. *Tectonophysics*, *450*(1–4), 34–50. https://doi.org/10.1016/j.tecto.2007.12.012

Wang, J., Kusky, T., Wang, L., Polat, A., & Deng, H. (2015). A Neoarchean subduction polarity reversal event in the North China Craton. *Lithos*, *220*, 133–146.

Willingshofer, E., Sokoutis, D., Luth, S. W., Beekman, F., & Cloetingh, S. (2013). Subduction and deformation of the continental lithosphere in response to plate and crust-mantle coupling. *Geology*, *41*(12), 1239–1242. https://doi.org/10.1130/G34815.1